



Impact of Thermally Dead Volume on Phonon Conduction along Silicon Nanoladders

Journal:	<i>Nanoscale</i>
Manuscript ID	NR-ART-03-2018-001788.R2
Article Type:	Paper
Date Submitted by the Author:	24-May-2018
Complete List of Authors:	<p>Park, Woosung; Stanford University, Mechanical Engineering Sohn, Joon; Stanford University, Electrical Engineering Romano, Giuseppe; Massachusetts Institute of Technology, Department of Mechanical Engineering Kodama, Takashi; Stanford University, Department of Mechanical Engineering Sood, Aditya; Stanford University, Materials Science and Engineering Katz, Joseph; Stanford University, Electrical Engineering Kim, Brian; Stanford University, Geballe Laboratory for Advanced Materials So, Hongyun; Hanyang University, Department of Mechanical Engineering Ahn, Ethan; The University of Texas at San Antonio, Department of Electrical and Computer Engineering Asheghi, Mehdi; Stanford University, Mechanical Engineering Kolpak, Alexie; Massachusetts Institute of Technology, Mechanical Engineering Goodson, Kenneth; Stanford University, Mechanical Engineering</p>

Impact of Thermally Dead Volume on Phonon Conduction along Silicon Nanoladders

Woosung Park,^{a,} Joon Sohn,^b Giuseppe Romano,^c Takashi Kodama,^a Aditya Sood,^{a,d} Joseph S. Katz,^{a,b} Brian S. Y. Kim,^e Hongyun So,^f Ethan C. Ahn,^g Mehdi Asheghi,^a Alexie M. Kolpak,^c and Kenneth E. Goodson^{a,*}*

^aDepartment of Mechanical Engineering, ^bDepartment of Electrical Engineering, Stanford University, Stanford, California 94305, USA

^cDepartment of Mechanical Engineering, Massachusetts Institute of Technology, Cambridge, Massachusetts 02139, USA

^dDepartment of Materials Science and Engineering, ^eGeballe Laboratory for Advanced Materials, Stanford University, Stanford, California 94305, USA

^fDepartment of Mechanical Engineering, Hanyang University, Seoul, 04763, South Korea

^gDepartment of Electrical and Computer Engineering, The University of Texas at San Antonio, 1 UTSA Circle, San Antonio, TX 78249, USA

Keywords: phonon conduction, ballistic phonon transport, thermal conductivity, phonon mean free paths, nanostructures

Abstract:

Thermal conduction in complex periodic nanostructures remains a key area of open questions and research, and a particularly provocative and challenging detail is the impact of nanoscale material volumes that do not lie along the optimal line of sight for conduction. Here, we experimentally study thermal transport in silicon nanoladders, which feature two orthogonal heat conduction paths: unobstructed line-of-sight channels in the axial direction and interconnecting bridges between them. The nanoladders feature an array of rectangular holes in a 10 μm long straight beam with a 970 nm wide and 75 nm thick cross-section. We vary the pitch of these holes from 200 nm to 1100 nm to modulate the contribution of bridges to the net transport of heat in the axial direction. The effective thermal conductivity, corresponding to reduced heat flux, decreases from $\sim 45 \text{ W m}^{-1} \text{ K}^{-1}$ to $\sim 31 \text{ W m}^{-1} \text{ K}^{-1}$ with decreasing pitch. By solving the Boltzmann transport equation using phonon mean free paths taken from *ab initio* calculations, we model thermal transport in the nanoladders, and experimental results show excellent agreement with the predictions to within $\sim 11\%$. A combination of experiments and calculations shows that with decreasing pitch, thermal transport in nanoladders approaches the counterpart in a straight beam equivalent to the line-of-sight channels, indicating that the bridges constitute a thermally dead volume. This study suggests that ballistic effects are dictated by the line-of-sight channels, providing key insights into thermal conduction in nanostructured metamaterials.

Introduction

Nanostructured materials have shown great promise in tuning key material characteristics, including optical,^{1, 2} mechanical,^{3, 4} and thermoelectric^{5, 6} properties. For example, ladder structures, a pair of wires connected to each other using orthogonal beams, have demonstrated significantly improved mechanical strength over that of a wire.^{7, 8} Nanostructures are often geometrically complex, requiring multiple characteristic lengths, e.g. dimensions for the orthogonal beams and wires in the ladders. In these complex structures, thermal transport is significantly suppressed due to boundary scattering when the length scales are comparable to mean free paths (MFPs) of energy carriers.^{9, 10} Despite much previous work on phonon-boundary scattering,^{11, 12} the impact of competing geometric length scales on phonon conduction still remains unclear.

For the present study, it is useful to view nanostructured materials in two groups: spatially continuous materials and porous media with discontinuity in mass. The continuous materials have constant cross-sections normal to the direction of the dominant temperature gradient, for example thin films^{13, 14}, nanowires¹⁵, and nanobeams.^{16, 17} Their thermal conductivities are reduced due to increased boundary scattering, and a theoretical model for phonon transport has been established using the ratio of a characteristic length and phonon MFPs.^{14, 16-21} In porous media, e.g. phononic crystals - thin films with nanoscopic holes in a periodic manner, nanoscale features increase phonon-boundary scattering as well as modify conduction paths.^{5, 22-24} The modification in the thermal paths causes inhomogeneous volumetric contributions to net heat flux, and the suppression in thermal conductivity is convolved with the inhomogeneity and the ballistic effects. Such spatial variations frequently occur at length scales comparable to the dominant phonon MFPs, leading to varying “local” definitions of thermal conductivity within different regions of the nanostructure^{5, 23, 25-27}. This increases the complexity of their experimental characterization. While it is generally accepted that the smallest feature size dictates the transport properties,²⁸⁻³⁰ understanding the details of the inhomogeneity is essential to identify and quantify other reduction mechanisms. Past studies on phononic crystal beams and films show that experimental results deviate from theoretical predictions,^{5, 23, 25, 26, 31, 32} leaving unanswered questions regarding conduction physics, such as the impacts of wave-like phonon behavior^{23, 25, 31} and roughness^{28, 33-35}. Such debates are partly attributed to incomplete understanding of the spatially varying ballistic effects since it is

difficult to decouple the effects of other mechanisms from that of boundary scattering. A key challenge for further investigation on conduction physics via nanostructures is to quantify the impact of inhomogeneous volumetric contribution on phonon-boundary scattering. Despite the importance of this topic, relevant systematic study is still absent.

Here, we present an experimental study of phonon transport in silicon nanoladders, which contain arrays of rectangular holes on the nanobeams creating spatially inhomogeneous contribution of heat-carrying ballistic phonons to net flux. As shown in Figure 1(a-f), the nanoladders comprise two major thermal conduction paths: necks along the free line-of-sight (LOS) channels and bridges that connect the parallel LOS paths orthogonally. We modulate the spacing between the holes to control the relative contribution of the bridges to the net thermal transport along the axial direction. We find that the thermal conductivity of the nanoladders is reduced with decreasing pitch of the holes, approaching the counterpart of an equivalent straight beam with the LOS channels. By calculating Boltzmann transport equation (BTE) with the bulk MFPs from *ab initio* calculations, we predict the thermal conductivity of nanoladders, showing agreement with the experimental results to within $\sim 11\%$.

Experimental

Silicon nanoladders are monolithically patterned between two suspended membranes using electron-beam lithography. An array of rectangular-shaped holes is introduced into a baseline reference sample, which is a $10\ \mu\text{m}$ long silicon ribbon with thickness $t \sim 75\ \text{nm}$ and width $w_{\text{Beam}} \sim 970\ \text{nm}$. The rectangular holes have width $w_{\text{Hole}} \sim 830\ \text{nm}$ and length $l_{\text{Hole}} \sim 130\ \text{nm}$. The spacing between holes, l_{Bridge} , is modulated. Specifically, we fabricate five different samples with l_{Bridge} of $\sim 70\ \text{nm}$, $\sim 170\ \text{nm}$, $\sim 270\ \text{nm}$, $\sim 470\ \text{nm}$ and $\sim 970\ \text{nm}$, as shown in Figure 1(a-f). We note that the surface roughness of the nanoladders is controlled to be the same across all the samples, as all features are patterned on the same wafer. Quasi-ballistic phonon flux maps show increasing contribution of the bridges to the net flux with increasing pitch as shown in Figure 1(b'-f') corresponding to the samples shown in Figure 1(b-f), respectively. The flux maps are obtained by calculating Boltzmann transport equation (BTE), and the details of this calculation are discussed below. The samples are fabricated on a silicon-on-insulator (SOI) wafer, and its device layer is doped with boron to a concentration of $\sim 10^{15}\ \text{cm}^{-3}$. Given the low dopant concentration

(corresponding to a resistivity of 14-22 $\Omega \cdot \text{cm}$), its impact on thermal transport is negligible.³⁶ The details of the sample fabrication are thoroughly described elsewhere.^{12, 16}

We use an electro-thermal characterization technique, which was originally developed for thermal measurements of nanomaterials, such as nanotubes and nanowires.^{37, 38} Briefly, heat is generated using Joule heating on one of the membranes, part of which is conducted through the nanobeam as depicted in Figure 2. Temperatures at both membranes are measured using resistive thermometry, and a temperature difference is controlled to be smaller than ~ 8 K. By measuring heat generation and temperatures at the hot and cold ends, we extract thermal conductance of the nanoladders, which is converted to thermal conductivity by solving the diffusive heat equation in COMSOL. All of the measurements are performed under vacuum to eliminate convection loss from both the platforms and nanobeam. The heat loss through radiation is negligible compared to other conduction channels.³⁸ The thermal boundary resistances between the heater/thermometers and the membranes are orders of magnitude smaller than the thermal resistance of the nanobeam test-section, and thus the interfacial resistances are neglected.³⁹ The experimental uncertainty is mainly attributed to the inaccuracy in the sample dimensions, which is inherent in the nanofabrication and scanning electron microscopy (SEM) measurements. The total measurement error in the thermal conductivity for all samples is estimated to be less than ~ 7 % (see Supporting Information).

Results and Discussion

We extract the effective thermal conductivity of the nanoladders, assuming uniform transport properties throughout the samples. With decreasing spacing l_{Bridge} , the effective thermal conductivity of nanoladders monotonically decreases from $\sim 45 \text{ W m}^{-1} \text{ K}^{-1}$ to $\sim 31 \text{ W m}^{-1} \text{ K}^{-1}$, as shown in Figure 3. The thermal conductivity is bounded by two limiting cases: 1) when l_{Bridge} approaches infinity, a reference beam with $w_{\text{Beam}} \sim 970 \text{ nm}$, and 2) when l_{Bridge} approaches zero, a straight beam with cross-section of $w_{\text{Beam}} \sim 70 \text{ nm}$. For both cases, the thickness is fixed at $t \sim 75 \text{ nm}$. The base reference of $l_{\text{Bridge}} \rightarrow \infty$, a straight beam with a cross-section of $w_{\text{Beam}} \sim 970 \text{ nm}$ and $t \sim 75 \text{ nm}$, is measured to be $\sim 51 \text{ W m}^{-1} \text{ K}^{-1}$, which agrees with literature and model predictions to within $\sim 2\%$ and 3% , respectively.¹⁶ The conduction through necks is limited by their cross-section,

which is ~ 70 nm wide and ~ 75 nm thick. The thermal conductivity of a straight beam equivalent to the necks is found to be ~ 33 W m⁻¹ K⁻¹ from literature.¹⁶ We note that the straight beam in the literature has a width $w_{\text{Beam}} \sim 65$ nm and thickness $t \sim 78$ nm, although the differences in dimensions have a negligible impact on the conductivity (see Supporting Information). The model prediction for the beam with $w_{\text{Beam}} \sim 70$ nm and $t \sim 75$ nm is ~ 35 W m⁻¹ K⁻¹, which agrees with the literature to within $\sim 6\%$. We note that the ladder with $l_{\text{Bridge}} = 70$ nm approaches the limiting case with $l_{\text{Bridge}} \rightarrow 0$ within experimental uncertainty. The variation in the conductivity between the two limiting cases indicates that bridges reduce phonon-boundary scattering sites with increasing hole spacing.

The actual heat flux is measured to be smaller than the model prediction in the diffusive transport regime while the contribution of the bridges to diffusive heat flux decreases with decreasing spacing (see Supporting Information). To understand the ballistic effects of the periodic holes, we model thermal transport in the nanoladders by solving the steady-state phonon BTE under the relaxation time approximation.⁴⁰ While the computational details are thoroughly documented elsewhere,⁴¹ we briefly describe the simulations here. The computations use a unit-cell consisting of a beam of width $w_{\text{Beam}} = 970$ nm, thickness $t = 75$ nm, and length $l_{\text{Unitcell}} = 3p$, where pitch $p = l_{\text{Bridge}} + l_{\text{Hole}}$. Periodic boundary conditions are applied on the boundaries in the direction of the temperature gradient with a temperature difference of $\Delta T = 1$ K. For the other boundaries, we assume diffuse boundary scattering at room temperature.⁴² The BTE is solved in space by the finite-volume method while the angular space is discretized by means of the discrete ordinate method. The BTE solver uses the phonon MFP spectra as its only input,⁴¹ which is computed by *ab initio* calculations from literature.¹⁰ For the phonons with isotropic distribution functions, we employ a modified diffusive equation, which enables accurate simulations and seamless integration with the BTE, with a reasonable spatial discretization.⁴¹

The effective conductivity for the nanoladders is calculated using a combination of bulk phonon MFPs, and the suppression function as given by⁹

$$k = \int_0^{\infty} S_{\Lambda}(\Lambda) f(\Lambda) d\Lambda \quad (1)$$

where f is the differential phonon MFP distribution for bulk silicon, S_{Λ} is the phonon suppression function, and Λ is an integration variable for phonon MFP in bulk silicon. The suppression function

S_Λ describes the suppression of heat flux carried by phonons with MFP Λ , and is obtained by solving the BTE in a given geometry.^{41, 43} The reduction in thermal conductivity corresponds to the reduced heat flux. The thermal conductivity is predicted for varying values of the spacing l_{Bridge} , and the prediction agrees with experimental results to within $\sim 11\%$ as shown in Figure 3. This agreement indicates that phonon suppression mechanisms are captured by the BTE calculation although the discrepancy between the measurements and the simulations for the ladders is larger than experimental uncertainties. We note that the model in this work does not include any fitting parameters while conventional methods include several fitting parameters. The model prediction also validates the use of diffuse scattering boundary conditions at room temperature.⁴² We also compare the direct calculations of BTE with a model using a ray-tracing method, which simulates phonon particles to estimate the reduced phonon MFPs in a given geometry (see Supporting Information).

By solving the BTE, we obtain heat flux maps as shown in Figure 2(b'-f'), which correspond to the samples in Figure 2(b-f). The maps show that heat flux is highly concentrated near the necks, and the heat spreading within the bridges decreases with decreasing bridge widths. (See Supporting Information for heat flux maps in the diffusive regime.) For the beam with $l_{\text{Bridge}} = 70$ nm, a minimal contribution of the bridges is observed. This observation is in agreement with previous research on two-dimensional phononic crystals, and films with microscopic holes, which showed a strong dependence of thermal conductivity only on their smallest dimension.^{5, 26} While heat spreading is limited only in the vicinity of the gap between necks in the case of $l_{\text{Bridge}} = 70$ nm, the sample with $l_{\text{Bridge}} = 970$ nm shows a significant amount of heat transfer within the bridges. Due to the decreasing contribution of the bridges to heat flux, the effective thermal conductivity of the nanoladders decreases by $\sim 24\%$ with decreasing spacing l_{Bridge} despite identical neck dimensions. This suppression in transport properties indicates that phonons are increasingly scattered from boundaries in bridges with decreasing spacing.

To understand the specific impact of the spacing between holes on the MFP spectrum, we calculate the thermal conductivity accumulation, which is given by⁴⁴

$$F(\Lambda_{bulk}) = \int_0^{\Lambda_{bulk}} S_{\Lambda}(\Lambda') f(\Lambda') d\Lambda' \quad (2)$$

The accumulation function is plotted as a function of bulk MFPs as shown in Figure 4. We compare the accumulation functions for nanoladders with l_{Bridge} from 70 nm to 970 nm, and the two limiting cases: straight beams with $w_{\text{Beam}} = 970$ nm (corresponding to $l_{\text{Bridge}} \rightarrow \infty$) and $w_{\text{Beam}} = 70$ nm (corresponding to $l_{\text{Bridge}} \rightarrow 0$). We define a bandwidth of MFPs that cover the transition from a regime of predominantly internal scattering to one of prevailing boundary scattering.¹² The bandwidth is set from a third of the characteristic length, $t/3$, to five times that, $5t$, where t is a thickness of the beam, representing a length scale for predominant boundary scattering.¹⁶ The accumulation is changed minimally for phonons with MFPs smaller than $t/3$, indicating diffusive phonon transport. For phonons with bulk MFPs in between $t/3$ and $5t$, the accumulations are mainly separated depending on l_{Bridge} , due to the impact of scattering from boundaries in bridges. The accumulations for phonons with $\Lambda_{\text{Bulk}} > 5t$ increase nearly in parallel for all samples despite appreciable contribution to the conductivity. The parallel increases show that these phonons are independent of scattering from boundaries in bridges, which suggests that substantial heat-carrying phonons travel through the LOS with minimal boundary scattering from sidewalls.^{12, 16}

It is also noteworthy that the accumulation function for the ladder with $l_{\text{Bridge}} = 970$ nm is closely overlapped with that for a straight beam with $w_{\text{Beam}} = 970$ nm, equivalent to $l_{\text{Bridge}} \rightarrow \infty$. This agreement indicates that ballistic effects due to bridges become increasingly negligible with increasing l_{Bridge} . In a straight beam with $w_{\text{Beam}} = 70$ nm, phonons with $\Lambda_{\text{Bulk}} > t$ are suppressed more strongly than the case of the ladder with $l_{\text{Bridge}} = 70$ nm. This indicates that phonons scatter more aggressively in a straight beam due to the completely enclosed boundaries along the LOS channel while open boundaries through bridges reduce scattering sites. Possible phonon scattering along the LOS channel is depicted in inset of Figure 4. The comparison between the ladder with $l_{\text{Bridge}} = 70$ nm and the straight beam with $w_{\text{Beam}} = 70$ nm suggests that the intersection between the LOS and bridges decreases scattering. This finding supports an increased possibility of other reduction mechanisms on nanomesh structures with periodic nanoscopic holes.^{23, 25, 27, 31, 32, 45}

Conclusions

In this work, we present experimental data for the thermal conductivity of ~ 75 nm thick silicon nanoladders with systematically controlled spacing between holes. The geometry serves to effectively isolate the volume between the slits, such that it contributes modestly to heat conduction. We solve the BTE based on MFP distributions for bulk silicon from *ab initio* calculations. A combination of experiments and calculations shows that thermal conductivity is bounded between a reference beam without any holes and a straight ribbon with equivalent LOS paths. The thermal conductivity accumulations also suggest that the intersection between necks and bridges increases boundary scattering from bridges, approaching that of the unobstructed LOS. This study has implications for the design of metamaterials through nanostructuring, such as in nanophotonics, nano-electromechanical systems, and microelectronics, where thermal transport plays an important role.

Conflicts of interest

There are no conflicts of interest to declare.

Acknowledgements

This work was supported by the National Science Foundation under grant No. 1336734. The work at UTSA was supported by the University of Texas System Faculty Science and Technology Acquisition and Retention (STARs) program. J.S.K. thanks the Semiconductor Research Corporation and the Intel Education Alliance for a Graduate Research Fellowship. Work at MIT was supported by the "Solid State Solar-Thermal Energy Conversion Center (S3TEC)," an Energy Frontier Research Center funded by the U.S. Department of Energy, Office of Science, Office of Basic Energy Sciences under Award No. DE-SC0001299/DE-FG02-09ER46577. Sample preparation and characterization were performed at the Stanford Nano Shared Facilities (SNSF), supported by the National Science Foundation under award ECCS-1542152.

Author contributions

W.P., M.A., and K.E.G. conceived the ideas for the project. W.P. designed and fabricated the experimental devices with help of J.S., T.K, E.C.A, and B.S.Y.K. W.P. performed the thermal conductivity measurements. G.R. performed Boltzmann transport model calculations under supervision of A.M.K. W.P. took scanning electron microscope. W.P., A.S., and B.S.Y.K, discussed experimental results and relevant physics. W.P. wrote the main manuscript text. J.S.K., A.S, B.S.Y.K, H.S, and K.E.G. commented on the manuscript. M.A. and K.E.G. guided the projects.

Supplementary Information

Additional information on uncertainty propagation of measurements, comparison in thermal transport models, and thermal transport in diffusive transport regime.

Corresponding Authors

Woosung Park (woosungpark@alumni.stanford.edu)

Kenneth E. Goodson (goodson@stanford.edu)

1. Y. Akahane, T. Asano, B.-S. Song and S. Noda, *Nature*, 2003, **425**, 944-947.
2. J. D. Joannopoulos, S. G. Johnson, J. N. Winn and R. D. Meade, *Photonic crystals: molding the flow of light*, Princeton university press, 2011.
3. L. R. Meza, S. Das and J. R. Greer, *Science*, 2014, **345**, 1322-1326.
4. M. D. Uchic, D. M. Dimiduk, J. N. Florando and W. D. Nix, *Science*, 2004, **305**, 986-989.
5. J. Tang, H.-T. Wang, D. H. Lee, M. Fardy, Z. Huo, T. P. Russell and P. Yang, *Nano Lett.*, 2010, **10**, 4279-4283.
6. K. W. Mauser, S. Kim, S. Mitrovic, D. Fleischman, R. Pala, K. C. Schwab and H. A. Atwater, *Nat. Nanotechnol.*, 2017, **12**, 770-775.
7. I. H. Shames and J. M. Pitarresi, *Introduction to solid mechanics*, Pearson College Division, 2000.
8. A. D. Schlüter, *Adv. Mater.*, 1991, **3**, 282-291.
9. A. J. Minnich, *Phys. Rev. Lett.*, 2012, **109**, 205901.
10. K. Esfarjani, G. Chen and H. T. Stokes, *Phys. Rev. B*, 2011, **84**, 085204.
11. D. G. Cahill, P. V. Braun, G. Chen, D. R. Clarke, S. Fan, K. E. Goodson, P. Keblinski, W. P. King, G. D. Mahan and A. Majumdar, *Appl. Phys. Rev.*, 2014, **1**, 011305.
12. W. Park, G. Romano, E. C. Ahn, T. Kodama, J. Park, M. T. Barako, J. Sohn, S. J. Kim, J. Cho and A. M. Marconnet, *Sci. Rep.*, 2017, **7**, 6233.
13. Y. Ju and K. Goodson, *Appl. Phys. Lett.*, 1999, **74**, 3005-3007.
14. M. Asheghi, M. Touzelbaev, K. Goodson, Y. Leung and S. Wong, *J. Heat Transfer*, 1998, **120**, 30-36.
15. D. Li, Y. Wu, P. Kim, L. Shi, P. Yang and A. Majumdar, *Appl. Phys. Lett.*, 2003, **83**, 2934-2936.
16. W. Park, D. D. Shin, S. J. Kim, J. S. Katz, J. Park, C. H. Ahn, T. Kodama, M. Asheghi, T. W. Kenny and K. E. Goodson, *Appl. Phys. Lett.*, 2017, **110**, 213102.
17. L. Yang, Y. Yang, Q. Zhang, Y. Zhang, Y. Jiang, Z. Guan, M. Gerboth, J. Yang, Y. Chen and D. G. Walker, *Nanoscale*, 2016, **8**, 17895-17901.
18. R. Chen, A. I. Hochbaum, P. Murphy, J. Moore, P. Yang and A. Majumdar, *Phys. Rev. Lett.*, 2008, **101**, 105501.
19. F. Alvarez and D. Jou, *Appl. Phys. Lett.*, 2007, **90**, 083109.

20. A. Sellitto, V. A. Cimmelli and D. Jou, in *Mesoscopic Theories of Heat Transport in Nanosystems*, Springer, 2016, pp. 1-30.
21. Y. Dong, B.-Y. Cao and Z.-Y. Guo, *Physica E Low Dimens Syst Nanostruct*, 2015, **66**, 1-6.
22. D. Song and G. Chen, *Appl. Phys. Lett.*, 2004, **84**, 687-689.
23. J.-K. Yu, S. Mitrovic, D. Tham, J. Varghese and J. R. Heath, *Nat. Nanotechnol.*, 2010, **5**, 718-721.
24. P. E. Hopkins, C. M. Reinke, M. F. Su, R. H. Olsson, E. A. Shaner, Z. C. Leseman, J. R. Serrano, L. M. Phinney and I. El-Kady, *Nano Lett.*, 2010, **11**, 107-112.
25. J. Lee, W. Lee, G. Wehmeyer, S. Dhuey, D. L. Olynick, S. Cabrini, C. Dames, J. J. Urban and P. Yang, *Nat. Commun.*, 2017, **8**, 14054.
26. J. Lim, H.-T. Wang, J. Tang, S. C. Andrews, H. So, J. Lee, D. H. Lee, T. P. Russell and P. Yang, *ACS Nano*, 2016, **10**, 124.
27. R. Anufriev, J. Maire and M. Nomura, *Phys. Rev. B*, 2016, **93**, 045411.
28. R. Yanagisawa, J. Maire, A. Ramiere, R. Anufriev and M. Nomura, *Appl. Phys. Lett.*, 2017, **110**, 133108.
29. M. Verdier, R. Anufriev, A. Ramiere, K. Termentzidis and D. Lacroix, *Phys. Rev. B*, 2017, **95**, 205438.
30. M. Nomura, Y. Kage, J. Nakagawa, T. Hori, J. Maire, J. Shiomi, R. Anufriev, D. Moser and O. Paul, *Phys. Rev. B*, 2015, **91**, 205422.
31. S. Alaie, D. F. Goettler, M. Su, Z. C. Leseman, C. M. Reinke and I. El-Kady, *Nat. Commun.*, 2015, **6**.
32. J. Maire, R. Anufriev, R. Yanagisawa, A. Ramiere, S. Volz and M. Nomura, *Sci. Adv.*, 2017, **3**, e1700027.
33. J. Lim, K. Hippalgaonkar, S. C. Andrews, A. Majumdar and P. Yang, *Nano Lett.*, 2012, **12**, 2475-2482.
34. A. I. Hochbaum, R. Chen, R. D. Delgado, W. Liang, E. C. Garnett, M. Najarian, A. Majumdar and P. Yang, *Nature*, 2008, **451**, 163-167.
35. M. G. Ghossoub, K. V. Valavala, M. Seong, B. Azeredo, K. Hsu, J. S. Sadhu, P. K. Singh and S. Sinha, *Nano Lett.*, 2013, **13**, 1564-1571.

36. M. Asheghi, K. Kurabayashi, R. Kasnavi and K. Goodson, *J. Appl. Phys.*, 2002, **91**, 5079-5088.
37. P. Kim, L. Shi, A. Majumdar and P. L. McEuen, *Phys. Rev. Lett.*, 2001, **87**, 215502.
38. L. Shi, D. LI, C. Yu, W. Jang, D. Kim, Z. Yao, P. Kim and A. Majumdar, *J. Heat Transfer*, 2003, **125**, 881-888.
39. K. Hippalgaonkar, B. Huang, R. Chen, K. Sawyer, P. Ercius and A. Majumdar, *Nano Lett.*, 2010, **10**, 4341-4348.
40. A. Joshi and A. Majumdar, *J. Appl. Phys.*, 1993, **74**, 31-39.
41. G. Romano and J. C. Grossman, *J. Heat Transfer*, 2015, **137**, 071302.
42. A. Vega-Flick, R. A. Duncan, J. K. Eliason, J. Cuffe, J. A. Johnson, J.-P. Peraud, L. Zeng, Z. Lu, A. A. Maznev and E. N. Wang, *AIP Advances*, 2016, **6**, 121903.
43. G. Romano and A. M. Kolpak, *Sci. Rep.*, 2017, **7**, 44379.
44. F. Yang and C. Dames, *Phys. Rev. B*, 2013, **87**, 35437-35443.
45. M. Nomura, J. Nakagawa, Y. Kage, J. Maire, D. Moser and O. Paul, *Appl. Phys. Lett.*, 2015, **106**, 143102.

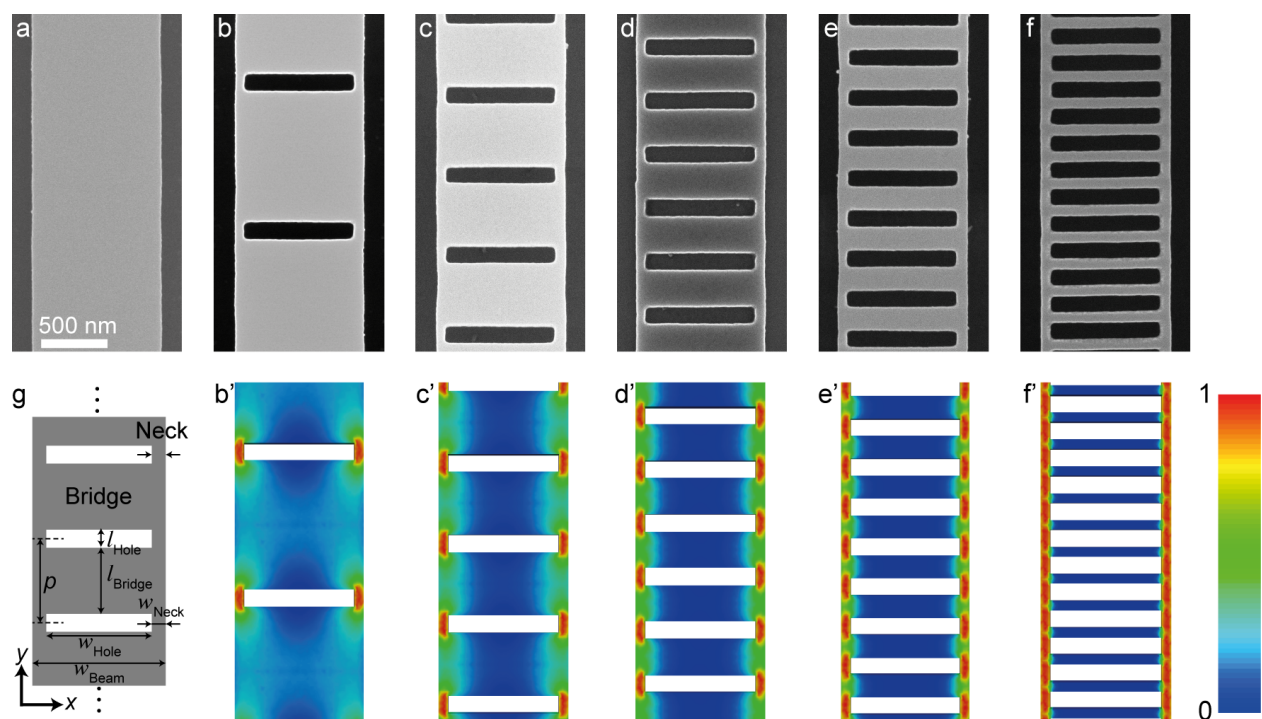


Figure 1. (a-f) Scanning electron microscopy (SEM) images of (a) a reference beam, $l_{\text{Bridge}} =$ (b) 970 nm, (c) 470 nm, (d) 270 nm, (e) 170 nm, and (f) 70 nm. (g) A schematic for the nanoladders, showing key geometric features and dimensions. (b'-f') Quasi-ballistic heat flux maps that are obtained by solving three-dimensional BTE, and the maps correspond to the sample (b-f), respectively. The heat flux maps are normalized per sample. The scale bar in (a) is shared through (a-f) and (b'-f').

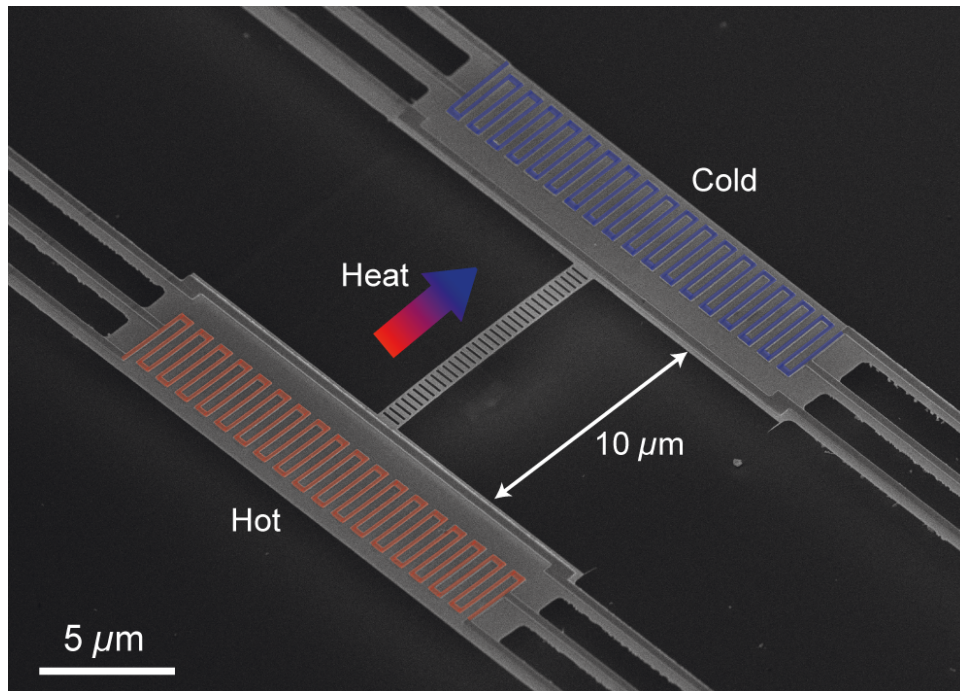


Figure 2. Image of the measurement structure, where a silicon nanoladder is connected between two suspended membranes. The resistive heater and thermometers are shown in false-color.

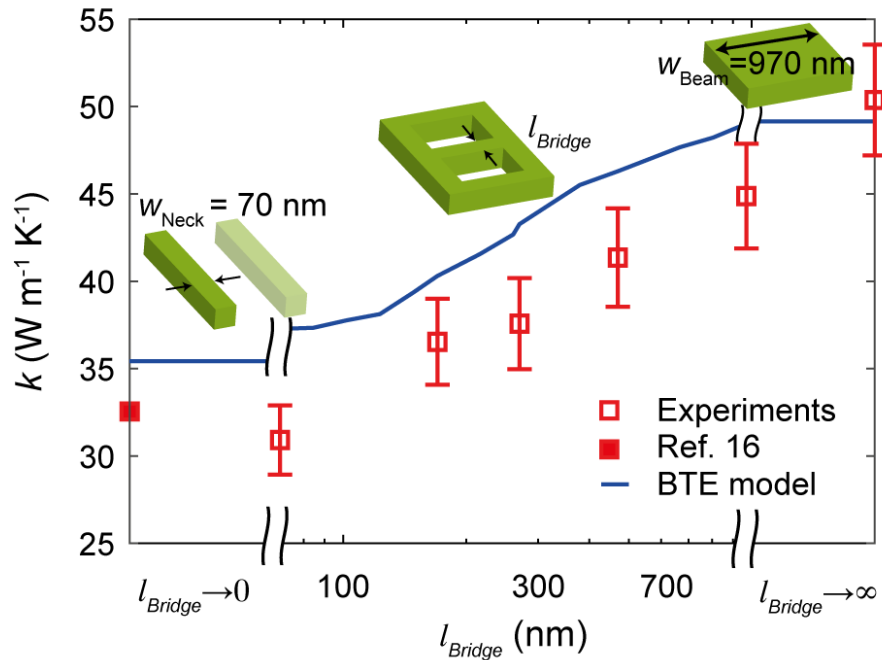


Figure 3. Thermal conductivity of the nanoladders as a function of spacing l_{Bridge} . Two limiting cases are also shown: straight beams with $w_{\text{Beam}} \sim 70$ nm and ~ 970 nm, each corresponding to l_{Bridge} approaching to zero and infinity, respectively. The thickness t is fixed to be ~ 75 nm. The thermal conductivity value for a straight beam with $w_{\text{Beam}} \sim 70$ nm is obtained from Ref. 16, where the cross-section is ~ 65 nm wide and ~ 78 nm thick. The blue solid line is the BTE model prediction obtained using Eq. 1. Insets show corresponding schematics with varying spacing l_{Bridge} .

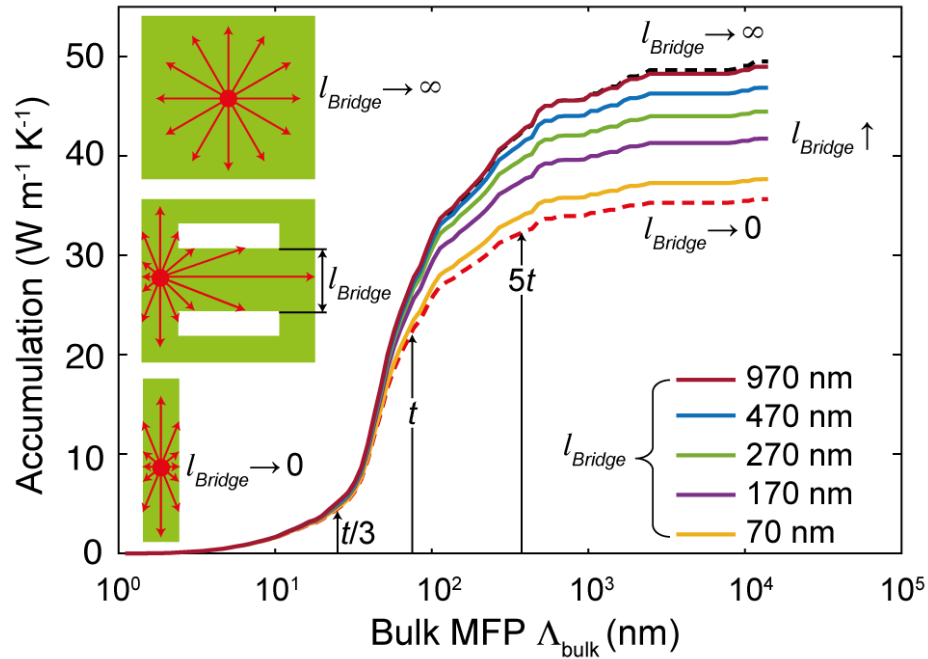
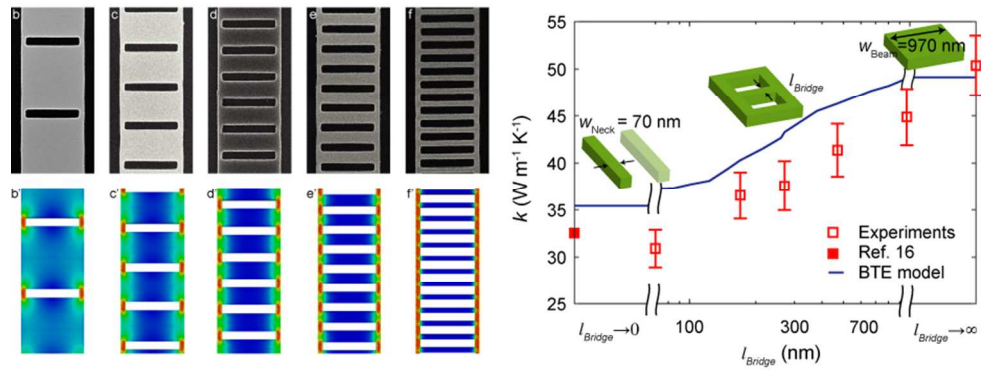


Figure 4. Accumulation of thermal conductivity as a function of bulk silicon mean free paths (MFPs) Λ_{bulk} . The black and red dashed lines indicate two limiting cases, $l_{\text{Bridge}} \rightarrow \infty$ and 0, which are equivalent to straight beams with $w_{\text{Beam}} = 970$ nm and 70 nm, respectively. The black solid arrows indicate the cases where Λ_{bulk} is equal to $t/3$, t , and $5t$, respectively, where t refers to beam thickness. Insets show schematics depicting possible phonon scattering from boundaries.

Silicon Nanoladders show that thermally dead volume minimally impacts on the ballistic effects.



81x30mm (300 x 300 DPI)